Quasi-analytical approximations and series in electromagnetic modeling

Michael S. Zhdanov*, Vladimir I. Dmitriev‡,
Sheng Fang**, and Gábor Hursán*

ABSTRACT

The quasi-linear approximation for electromagnetic forward modeling is based on the assumption that the anomalous electrical field within an inhomogeneous domain is linearly proportional to the background (normal) field through an electrical reflectivity tensor $\hat{\lambda}$. In the original formulation of the quasi-linear approximation, $\hat{\lambda}$ was determined by solving a minimization problem based on an integral equation for the scattering currents. This approach is much less time-consuming than the full integral equation method; however, it still requires solution of the corresponding system of linear equations. In this paper, we present a new approach to the approximate solution of the integral equation using $\hat{\lambda}$ through construction of quasi-analytical expressions for the anomalous electromagnetic field for 3-D and 2-D models. Quasi-analytical solutions reduce dramatically the computational effort related to forward electromagnetic modeling of inhomogeneous geoelectrical structures. In the last sections of this paper, we extend the quasi-analytical method using iterations and develop higher order approximations resulting in quasi-analytical series which provide improved accuracy. Computation of these series is based on repetitive application of the given integral contraction operator, which insures rapid convergence to the correct result. Numerical studies demonstrate that quasi-analytical series can be treated as a new powerful method of fast but rigorous forward modeling solution.

INTRODUCTION

The integral equation (IE) method is a powerful tool for electromagnetic numerical modeling (Hohmann, 1975; Weidelt, 1975; Dmitriev and Pozdnyakova, 1992). This method is based on expressing the electromagnetic fields in terms of an integral equation with respect to the excess current within an inhomogeneity. The integral equation is written as a system of linear algebraic equations by approximating the excess current distribution $\mathbf{j}^a$ by the piecewise constant functions. The resulting algebraic system is solved numerically (Xiong, 1992). The main difficulty of this technique is the size of the linear system of equations matrix, which demands excessive computer memory and calculation time to invert. This limitation of the integral equation technique becomes critical in inverse problem solution which requires multiple forward modeling calculations for different (updated) geoelectrical model parameters.

A novel approach to 3-D electromagnetic (EM) modeling based on linearization of the integral equations for scattered EM fields has been developed recently by Zhdanov and Fang (1996a, b, 1997). Within this method, called quasi-linear (QL) approximation, the excess currents are assumed to be proportional to the background (normal) field $\mathbf{E^b}$ through an electrical reflectivity tensor $\hat{\lambda}$. In the original papers on QL approximations, the electrical reflectivity tensor was determined by solving a minimization problem based on an integral equation for the scattering currents (Zhdanov and Fang, 1996a, b). This problem is much less time-consuming than the full IE method; however, it still requires solution of the corresponding system of linear equations. In this paper, we present a new approach to estimating $\hat{\lambda}$, which leads to constructing quasi-analytical (QA) expressions for the anomalous electromagnetic field for 3-D and 2-D models. We demonstrate also the connection between the QL and QA approximations and the localized nonlinear (LN) approximations introduced by Habashy et al. (1993) and Torres-Verdin and Habashy (1994) and conduct a comparative study of the accuracy of different approximations.

In the last sections of the paper, we extend the quasi-analytical method using iterative techniques and develop

approximations of the higher orders which provide better accuracy than the original QA and LN approximations. Combination of these iterative solutions forms the quasi-analytical series which generate a rigorous solution of EM modeling problems.

TENSOR QUASI-LINEAR EQUATION

Consider a 3-D geoelectric model with the background (normal) complex conductivity $\tilde{\sigma}_b$ and local inhomogeneity $\mathbf{D}$ with the arbitrary spatial variations of complex conductivity $\tilde{\sigma} = \tilde{\sigma}_b + \Delta\tilde{\sigma}$. We assume that $\mu = \mu_0 = 4\pi \times 10^{-7}$ H/m, where μ_0 is the free-space magnetic permeability. The model is excited by an electromagnetic field generated by an arbitrary source time harmonic as $e^{-i\omega t}$. Complex conductivity includes the effect of displacement currents: $\tilde{\sigma} = \sigma - i\omega\varepsilon$, where σ and ε are electrical conductivity and dielectric permittivity. The electromagnetic fields in this model can be expressed as a sum of the background (normal) and anomalous fields:

$$\mathbf{E} = \mathbf{E}^b + \mathbf{E}^a, \qquad \mathbf{H} = \mathbf{H}^b + \mathbf{H}^a, \qquad (1)$$

where the background field is a field generated by the given sources in the model with the background distribution of conductivity $\tilde{\sigma}_b$, and the anomalous field is produced by the anomalous conductivity distribution $\Delta\tilde{\sigma}$.

It is well known that the anomalous field can be presented as an integral over the excess currents in inhomogeneous domain $\mathbf{D}$ (Hohmann, 1975; Weidelt, 1975):

$$\mathbf{E}^a(\mathbf{r}_j) = \iiint_{\mathbf{D}} \hat{\mathbf{G}}_E(\mathbf{r}_j \mid \mathbf{r})\mathbf{j}^a(\mathbf{r}) \, d\mathbf{v} = \mathbf{G}_E(\mathbf{j}^a),$$
$$\mathbf{H}^a(\mathbf{r}_j) = \iiint_{\mathbf{D}} \hat{\mathbf{G}}_H(\mathbf{r}_j \mid \mathbf{r})\mathbf{j}^a(\mathbf{r}) \, d\mathbf{v} = \mathbf{G}_H(\mathbf{j}^a), \qquad (2)$$

where $\hat{\mathbf{G}}_E(\mathbf{r}_j \mid \mathbf{r})$ and $\hat{\mathbf{G}}_H(\mathbf{r}_j \mid \mathbf{r})$ are, respectively, the electric and magnetic Green's tensors defined for an unbounded conductive medium with the background conductivity $\tilde{\sigma}_b$, $\mathbf{G}_E$ and $\mathbf{G}_H$ are the corresponding Green's linear operators, and excess current $\mathbf{j}^a$ is determined by the equation

$$\mathbf{j}^a = \Delta\tilde{\sigma}\mathbf{E} = \Delta\tilde{\sigma}(\mathbf{E}^b + \mathbf{E}^a). \qquad (3)$$

Using Green's operators, one can calculate the electromagnetic field at any point $\mathbf{r}_j$, if the electric field is known within the inhomogeneity:

$$\mathbf{E}(\mathbf{r}_j) = \mathbf{G}_E(\Delta\tilde{\sigma}\mathbf{E}) + \mathbf{E}^b(\mathbf{r}_j), \qquad (4)$$
$$\mathbf{H}(\mathbf{r}_j) = \mathbf{G}_H(\Delta\tilde{\sigma}\mathbf{E}) + \mathbf{H}^b(\mathbf{r}_j). \qquad (5)$$

Expression (4) becomes the integral equation with respect to electric field $\mathbf{E}(\mathbf{r})$, if $\mathbf{r}_j \in \mathbf{D}$.

The QL approximation is based on the assumption that the anomalous field $\mathbf{E}^a$ inside the inhomogeneous domain is linearly proportional to the background field $\mathbf{E}^b$ through some tensor $\hat{\lambda}$ (Zhdanov and Fang, 1996a):

$$\mathbf{E}^a(\mathbf{r}) \approx \hat{\lambda}(\mathbf{r})\mathbf{E}^b(\mathbf{r}). \qquad (6)$$

Substituting formula (6) into formula (4), we obtain the QL approximation $\mathbf{E}^a_{q1}(\mathbf{r})$ for the anomalous field:

$$\mathbf{E}^a_{q1}(\mathbf{r}_j) = \mathbf{G}_E(\Delta\tilde{\sigma}(\hat{\mathbf{I}} + \hat{\lambda}(\mathbf{r}))\mathbf{E}^b). \qquad (7)$$

Rewriting expression (7) gives the tensor quasi-linear (TQL) equation with respect to the electrical reflectivity tensor $\hat{\lambda}$:

$$\hat{\lambda}(\mathbf{r}_j)\mathbf{E}^b(\mathbf{r}_j) = \mathbf{G}_E[\Delta\tilde{\sigma}\hat{\lambda}(\mathbf{r})\mathbf{E}^b] + \mathbf{E}^B(\mathbf{r}_j), \qquad (8)$$

where $\mathbf{E}^B(\mathbf{r}_j)$ denotes the Born approximation:

$$\mathbf{E}^B(\mathbf{r}_j) = \mathbf{G}_E(\Delta\tilde{\sigma}\mathbf{E}^b) = \int_{\mathbf{D}} \hat{\mathbf{G}}_E(\mathbf{r}_j \mid \mathbf{r})\Delta\tilde{\sigma}(\mathbf{r})\mathbf{E}^b(\mathbf{r}) \, d\mathbf{v}, \qquad (9)$$

and $\mathbf{G}_E[\Delta\tilde{\sigma}\hat{\lambda}(\mathbf{r})\mathbf{E}^b]$ is a linear operator of $\hat{\lambda}(\mathbf{r})$:

$$\mathbf{G}_E[\Delta\tilde{\sigma}\hat{\lambda}(\mathbf{r})\mathbf{E}^b] = \int_{\mathbf{D}} \hat{\mathbf{G}}_E(\mathbf{r}_j \mid \mathbf{r})\Delta\sigma(\mathbf{r})\hat{\lambda}(\mathbf{r})\mathbf{E}^b(\mathbf{r}) \, d\mathbf{v}. \qquad (10)$$

The original QL approximation (Zhdanov and Fang, 1996a, b) was based on the numerical solution of a minimization problem arising from the TQL equation (8):

$$\left\| \hat{\lambda}(\mathbf{r}_j)\mathbf{E}^b(\mathbf{r}_j) - \mathbf{G}_E[\Delta\tilde{\sigma}\hat{\lambda}(\mathbf{r})\mathbf{E}^b] - \mathbf{E}^B(\mathbf{r}_j) \right\| = \min. \qquad (11)$$

The advantage of this approach is that, by choosing a fine enough discretization for a function $\hat{\lambda}(\mathbf{r}_j)$, one can generate an accurate solution. The disadvantage, however, is that similar to the full IE method, the QL approach still requires solution of the corresponding system of linear equations. In this paper, we develop a new TQL equation solution that results in analytical expressions for the electrical reflectivity tensor $\hat{\lambda}(\mathbf{r}_j)$. This technique is, obviously, much faster than the original QL approximation. However, it may be less accurate than the corresponding QL approximation with a fine grid for $\hat{\lambda}(\mathbf{r}_j)$ discretization. In other words, there is a trade-off between the simplicity of the approximate solution and its accuracy.

QUASI-ANALYTICAL SOLUTIONS FOR 3-D ELECTROMAGNETIC FIELD

In this section we analyze different approximate solutions of the TQL equation (8). The iterative approach to the rigorous solution of the TQL equation is outlined in Appendix A.

Solution for a scalar reflectivity tensor

In the framework of the quasi-linear approach, we may consider the electrical reflectivity tensor selected to be a scalar (Zhdanov and Fang, 1996a), $\hat{\lambda} = \lambda\hat{\mathbf{I}}$, where $\hat{\mathbf{I}}$ is the unity tensor. In this case, integral equation (8) can be rewritten as

$$\lambda(\mathbf{r}_j)\mathbf{E}^b(\mathbf{r}_j) = \mathbf{G}_E[\Delta\tilde{\sigma}\lambda\mathbf{E}^b] + \mathbf{E}^B(\mathbf{r}_j). \qquad (12)$$

Following Habashy et al. (1993) and Torres-Verdin and Habashy (1994), we note that Green's tensor $\hat{\mathbf{G}}_E(\mathbf{r}_j \mid \mathbf{r})$ is singular at the point where $\mathbf{r}_j = \mathbf{r}$. Therefore, one can expect that the dominant contribution to the integral $\mathbf{G}_E[\Delta\tilde{\sigma}\lambda\mathbf{E}^b]$ in equation (12) is from some vicinity of the point $\mathbf{r}_j = \mathbf{r}$. Assuming that $\lambda(\mathbf{r}_j)$ is slowly varying within domain $\mathbf{D}$, we write

$$\lambda(\mathbf{r}_j)\mathbf{E}^b(\mathbf{r}_j) \approx \lambda(\mathbf{r}_j)\mathbf{G}_E[\Delta\tilde{\sigma}\mathbf{E}^b] + \mathbf{E}^B(\mathbf{r}_j)$$
$$= \lambda(\mathbf{r}_j)\mathbf{E}^B(\mathbf{r}_j) + \mathbf{E}^B(\mathbf{r}_j). \qquad (13)$$

As we seek a scalar reflectivity coefficient λ, it is useful to calculate the dot product of both sides of equation (13) and the

background electric field:

$$\lambda(\mathbf{r_j})\mathbf{E^b}(\mathbf{r_j}) \cdot \mathbf{E^b}(\mathbf{r_j})$$
$$= \lambda(\mathbf{r_j})\mathbf{E^B}(\mathbf{r_j}) \cdot \mathbf{E^b}(\mathbf{r_j}) + \mathbf{E^B}(\mathbf{r_j}) \cdot \mathbf{E^b}(\mathbf{r_j}). \quad (14)$$

Assuming that

$$\mathbf{E^b}(\mathbf{r_j}) \cdot \mathbf{E^b}(\mathbf{r_j}) \neq 0, \quad (15)$$

and dividing equation (14) by the square of the background field, we obtain

$$\lambda(\mathbf{r_j}) = \frac{g(\mathbf{r_j})}{1 - g(\mathbf{r_j})}, \quad (16)$$

where

$$g(\mathbf{r_j}) = \frac{\mathbf{E^B}(\mathbf{r_j}) \cdot \mathbf{E^b}(\mathbf{r_j})}{\mathbf{E^b}(\mathbf{r_j}) \cdot \mathbf{E^b}(\mathbf{r_j})}. \quad (17)$$

Substituting equation (16) into equation (1), we find

$$\mathbf{E}(\mathbf{r}) = \mathbf{E^a}(\mathbf{r}) + \mathbf{E^b}(\mathbf{r}) \approx [\lambda(\mathbf{r}) + 1]\mathbf{E^b}(\mathbf{r})$$
$$= \frac{1}{1 - g(\mathbf{r})}\mathbf{E^b}(\mathbf{r}). \quad (18)$$

Therefore from equations (4) and (5), we finally determine

$$\mathbf{E^a_{QA}}(\mathbf{r_j}) = \mathbf{E}(\mathbf{r_j}) - \mathbf{E^b}(\mathbf{r_j})$$
$$= \iiint_D \hat{\mathbf{G}}_E(\mathbf{r_j} \,|\, \mathbf{r})\frac{\Delta\tilde{\sigma}(\mathbf{r})}{1 - g(\mathbf{r})}\mathbf{E^b}(\mathbf{r})\, \mathbf{dv}, \quad (19)$$

and

$$\mathbf{H^a_{QA}}(\mathbf{r_j}) = \mathbf{H}(\mathbf{r_j}) - \mathbf{H^b}(\mathbf{r_j})$$
$$= \iiint_D \hat{\mathbf{G}}_H(\mathbf{r_j} \,|\, \mathbf{r})\frac{\Delta\tilde{\sigma}(\mathbf{r})}{1 - g(\mathbf{r})}\mathbf{E^b}(\mathbf{r})\, \mathbf{dv}. \quad (20)$$

Formulas (19) and (20) give QA solutions for 3-D electromagnetic fields. Note that the only difference between the new QA approximation and the Born approximation (9) is the presence of the scalar function $[1 - g(\mathbf{r})]^{-1}$. Hence computationally, the QA approximation and the Born approximation are practically the same. On the other hand, we show below that the QA approximation is more accurate than the Born approximation.

General solution for different polarizations of the anomalous and background electric fields

The QA solutions developed in the previous section were based on the assumption that the electrical reflectivity was a scalar. This assumption reduces the areas of practical application of the QA approximations because in this case the anomalous (scattered) field is polarized in direction parallel to the background field within the inhomogeneity. However, in general, the anomalous field can be polarized in a different direction than the background field. To overcome this difficulty, we introduce a tensor quasi-analytical (TQA) approximation to $\hat{\lambda}$, which permits different polarizations for the background and anomalous (scattered) fields.

We again assume that the product $\hat{\lambda}(\mathbf{r})\mathbf{E^b}(\mathbf{r})$ is a smoothly varying function of the coordinates, and it can be taken outside

the integral over the anomalous domain $\mathbf{D}$ without substantial discrepancies. As a result, we obtain from the TQL equation (8)

$$\hat{\lambda}(\mathbf{r_j})\mathbf{E^b}(\mathbf{r_j}) \approx \mathbf{G}_E[\Delta\tilde{\sigma}\hat{\mathbf{I}}]\hat{\lambda}(\mathbf{r_j})\mathbf{E^b}(\mathbf{r_j}) + \mathbf{E^B}(\mathbf{r_j})$$
$$= \hat{\mathbf{g}}(\mathbf{r_j})\hat{\lambda}(\mathbf{r_j})\mathbf{E^b}(\mathbf{r_j}) + \mathbf{E^B}(\mathbf{r_j}),$$

or

$$[\hat{\mathbf{I}} - \hat{\mathbf{g}}(\mathbf{r_j})]\hat{\lambda}(\mathbf{r_j})\mathbf{E^b}(\mathbf{r_j}) = \mathbf{E^B}(\mathbf{r_j}), \quad (21)$$

where

$$\hat{\mathbf{g}}(\mathbf{r_j}) = \mathbf{G}_E[\Delta\tilde{\sigma}(\mathbf{r})\hat{\mathbf{I}}].$$

Solving equation (21) yields

$$\hat{\lambda}(\mathbf{r_j})\mathbf{E^b}(\mathbf{r_j}) = [\hat{\mathbf{I}} - \hat{\mathbf{g}}(\mathbf{r_j})]^{-1}\mathbf{E^B}(\mathbf{r_j}). \quad (22)$$

Substituting equation (22) into equation (1), we obtain

$$\mathbf{E}(\mathbf{r}) = \mathbf{E^a}(\mathbf{r}) + \mathbf{E^b}(\mathbf{r}) \approx [\hat{\lambda}(\mathbf{r}) + \hat{\mathbf{I}}]\mathbf{E^b}(\mathbf{r})$$
$$= [\hat{\mathbf{I}} - \hat{\mathbf{g}}(\mathbf{r})]^{-1}\mathbf{E^B}(\mathbf{r}) + \mathbf{E^b}(\mathbf{r}). \quad (23)$$

Therefore, from equations (4) and (5) we find

$$\mathbf{E^a_{TQA}}(\mathbf{r_j}) = \mathbf{E}(\mathbf{r_j}) - \mathbf{E^b}(\mathbf{r_j}) = \iiint_D \hat{\mathbf{G}}_E(\mathbf{r_j} \,|\, \mathbf{r})\Delta\tilde{\sigma}(\mathbf{r})$$
$$\times \{[\hat{\mathbf{I}} - \hat{\mathbf{g}}(\mathbf{r})]^{-1}\mathbf{E^B}(\mathbf{r}) + \mathbf{E^b}(\mathbf{r})\}\, dv, \quad (24)$$

and

$$\mathbf{H^a_{TQA}}(\mathbf{r_j}) = \mathbf{H}(\mathbf{r_j}) - \mathbf{H^b}(\mathbf{r_j}) = \iiint_D \hat{\mathbf{G}}_H(\mathbf{r_j} \,|\, \mathbf{r})\Delta\tilde{\sigma}(\mathbf{r})$$
$$\times \{[\hat{\mathbf{I}} - \hat{\mathbf{g}}(\mathbf{r})]^{-1}\mathbf{E^B}(\mathbf{r}) + \mathbf{E^b}(\mathbf{r})\}\, dv, \quad (25)$$

where

$$\hat{\mathbf{g}}(\mathbf{r_j}) = \mathbf{G}_E[\Delta\tilde{\sigma}(\mathbf{r})\hat{\mathbf{I}}] = \iiint_D \hat{\mathbf{G}}_E(\mathbf{r_j} \,|\, \mathbf{r})\Delta\tilde{\sigma}(\mathbf{r})\, \mathbf{dv}. \quad (26)$$

We call expressions (24) and (25) TQA approximations for an electromagnetic field. We show below that this approximation provides a more accurate solution for a forward problem than a scalar QA approximation. However, we must compute the tensor multiplier $[\hat{\mathbf{I}} - \hat{\mathbf{g}}(\mathbf{r})]^{-1}$, which is slightly more time-consuming than calculation of the scalar coefficient $[1 - g(\mathbf{r})]^{-1}$.

Quasi-analytical solutions for a 2-D electromagnetic field

Assume now that both the electromagnetic field and the complex conductivity $\tilde{\sigma}$ in the geoelectrical model are two-dimensional (i.e., they vary only along the directions x and z of some Cartesian system of coordinates, and are constant in the y direction). In this case, repeating derivations described above for the 3-D case, we can obtain the following QA expressions for a 2-D electromagnetic field:

$$E^a_{QAy}(\mathbf{r_j}) \approx i\omega\mu_0 \iint_D G_b(\mathbf{r_j} \,|\, \mathbf{r})\frac{\Delta\tilde{\sigma}(\mathbf{r})}{1 - g(\mathbf{r})}E^b_y(\mathbf{r})\, ds, \quad (27)$$

and similarly for magnetic field components:

$$H_{QAx}^a(\mathbf{r_j}) \approx -\iint_D \frac{\partial G_b(\mathbf{r_j}|\mathbf{r})}{\partial z} \frac{\Delta \tilde{\sigma}(\mathbf{r})}{1 - g(\mathbf{r})} E_y^b(\mathbf{r}) \, ds, \quad (28)$$

$$H_{QAz}^a(\mathbf{r_j}) \approx -\iint_D \frac{\partial G_b(\mathbf{r_j}|\mathbf{r})}{\partial x} \frac{\Delta \tilde{\sigma}(\mathbf{r})}{1 - g(\mathbf{r})} E_y^b(\mathbf{r}) \, ds, \quad (29)$$

where $G_b(\mathbf{r_j}|\mathbf{r})$ is a 2-D scalar Green's function for an unbounded conductive medium with the background conductivity $\tilde{\sigma}_b$, and

$$g(\mathbf{r}) = \frac{E_y^B(\mathbf{r})}{E_y^b(\mathbf{r})}. \quad (30)$$

These formulas can serve as a new effective QA tool for both direct and inverse 2-D electromagnetic problem solutions. Numerical tests demonstrate that these approximations produce a very accurate result for 2-D models (Dmitriev et al., 1998).

LOCALIZED NONLINEAR APPROXIMATION

The TQA approximation can be treated as a generalization of the LN approximation introduced by Habashy et al. (1993). Let us rewrite equation (23) in the form

$$\mathbf{E}(\mathbf{r}) = [\hat{\mathbf{I}} - \hat{\mathbf{g}}(\mathbf{r})]^{-1}[\mathbf{E}^\mathbf{B}(\mathbf{r}) - \hat{\mathbf{g}}(\mathbf{r})\mathbf{E}^\mathbf{b}(\mathbf{r})]$$
$$+ [\hat{\mathbf{I}} - \hat{\mathbf{g}}(\mathbf{r})]^{-1}\mathbf{E}^\mathbf{b}(\mathbf{r}). \quad (31)$$

Taking into account once again that Green's tensor $\hat{\mathbf{G}}_E(\mathbf{r_j}|\mathbf{r})$ exhibits either singularity or a peak at the point where $\mathbf{r_j} = \mathbf{r}$, one can calculate the Born approximation $\mathbf{G_E}[\Delta \tilde{\sigma}(\mathbf{r})\mathbf{E}^\mathbf{b}(\mathbf{r})]$ using the formula

$$\mathbf{E}^\mathbf{B}(\mathbf{r_j}) = \mathbf{G_E}[\Delta \tilde{\sigma}(\mathbf{r})\mathbf{E}^\mathbf{b}(\mathbf{r})] \approx \hat{\mathbf{g}}(\mathbf{r_j})\mathbf{E}^\mathbf{b}(\mathbf{r_j}).$$

This result implies

$$\mathbf{E}^\mathbf{B}(\mathbf{r}) - \hat{\mathbf{g}}(\mathbf{r})\mathbf{E}^\mathbf{b}(\mathbf{r}) \approx \mathbf{0}, \quad (32)$$

and is particularly appropriate if the background field is a smoothly varying spatial function (Habashy et al., 1993).

Under assumption (32), equation (31) can be rewritten

$$\mathbf{E}(\mathbf{r}) = \mathbf{E}^\mathbf{a}(\mathbf{r}) + \mathbf{E}^\mathbf{b}(\mathbf{r}) \approx [\hat{\mathbf{I}} - \hat{\mathbf{g}}(\mathbf{r})]^{-1}\mathbf{E}^\mathbf{b}(\mathbf{r}). \quad (33)$$

Therefore, from equations (4) and (5) we find

$$\mathbf{E}_{LN}^\mathbf{a}(\mathbf{r_j}) = \mathbf{E}(\mathbf{r_j}) - \mathbf{E}^\mathbf{b}(\mathbf{r_j})$$
$$= \iiint_D \hat{\mathbf{G}}_E(\mathbf{r_j}|\mathbf{r})\Delta \tilde{\sigma}(\mathbf{r})[\hat{\mathbf{I}} - \hat{\mathbf{g}}(\mathbf{r})]^{-1}\mathbf{E}^\mathbf{b}(\mathbf{r}) \, \mathbf{dv}, \quad (34)$$

and

$$\mathbf{H}_{LN}^\mathbf{a}(\mathbf{r_j}) = \mathbf{H}(\mathbf{r_j}) - \mathbf{H}^\mathbf{b}(\mathbf{r_j})$$
$$= \iiint_D \hat{\mathbf{G}}_H(\mathbf{r_j}|\mathbf{r})\Delta \tilde{\sigma}(\mathbf{r})[\hat{\mathbf{I}} - \hat{\mathbf{g}}(\mathbf{r})]^{-1}\mathbf{E}^\mathbf{b}(\mathbf{r}) \, \mathbf{dv}. \quad (35)$$

Formulas (34) and (35) express the LN approximation introduced by Habashy et al. (1993), where

$$[\hat{\mathbf{I}} - \hat{\mathbf{g}}(\mathbf{r})]^{-1} = \hat{\mathbf{\Gamma}}(\mathbf{r})$$

is their depolarization tensor.

Thus we can see that the difference between the TQL approximation and the LN approximation is determined by a term

$$\mathbf{E}_{TQA}^\mathbf{a}(\mathbf{r_j}) - \mathbf{E}_{LN}^\mathbf{a}(\mathbf{r_j})$$
$$= \iiint_D \hat{\mathbf{G}}_E(\mathbf{r_j}|\mathbf{r})\Delta \tilde{\sigma}(\mathbf{r})\hat{\mathbf{\Gamma}}(\mathbf{r})[\mathbf{E}^\mathbf{B}(\mathbf{r}) - \hat{\mathbf{g}}(\mathbf{r})\mathbf{E}^\mathbf{b}(\mathbf{r})] \, dv. \quad (36)$$

Note that both TQA and LN approximations use the same depolarization tensor $\hat{\mathbf{\Gamma}}(\mathbf{r})$, based on the idea of a localized effect in the Green's integral operator. The only difference is that in the case of the LN approximation we use this localization property twice for computing both the depolarization tensor and the expression for the Born approximation $\mathbf{E}^\mathbf{B}(\mathbf{r_j})$ on the right-hand side of the TQL equation (8). In the case of TQA approximation, we use the exact formula for $\mathbf{E}^\mathbf{B}(\mathbf{r_j})$, and we consider TQA a partially localized approximation. This difference does affect the accuracy of these two approximations for different geoelectrical models, illustrated below by numerical examples.

COMPARATIVE ACCURACY STUDY

To compare the accuracy of the Born, QA, TQA, and LN approximations, we conducted several numerical experiments for the models presented in Figure 1. Model 1 consists of a conductive rectangular prism embedded in a homogeneous half-space excited by a horizontal rectangular loop (Figure 1, top panel).
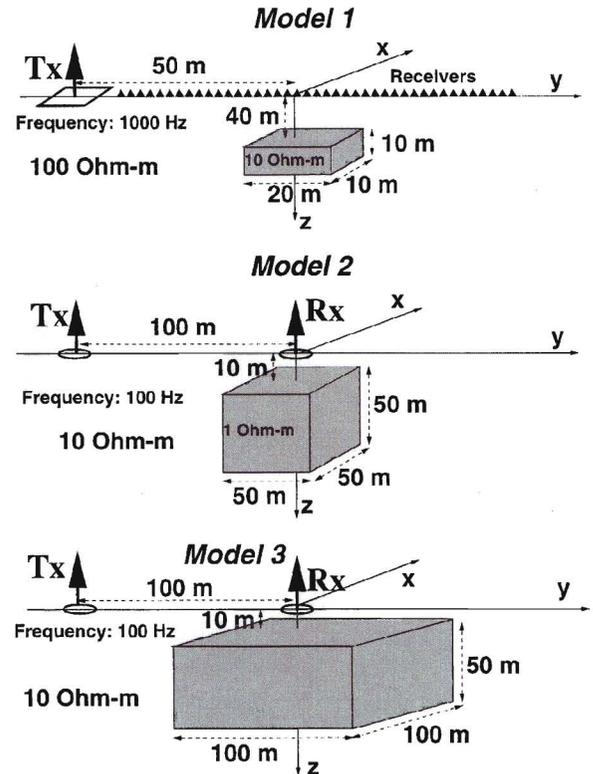
FIG. 1. 3-D geoelectrical models used for comparative accuracy study of different approximations.

The frequency is 1000 Hz, and the conductivity ratio is 10. The receivers are located above the body along the y-axis. Model 2 consists of a conductive cube with a resistivity of 1 ohm-m located at a depth of 10 m within a homogeneous half-space with a resistivity of 10 ohm-m (Figure 1, middle panel). The sides of the cubic prism have a length of 50 m. Model 3 contains the body with a horizontal size of 100 m × 100 m, a vertical dimension of 50 m, and located at a depth of 10 m. The EM field in models 2 and 3 is excited by a vertical magnetic dipole located on the surface of the earth.

Figure 2 shows the real and imaginary parts of the horizontal electric and vertical magnetic components of the scattered field computed by solving the full integral equation and the approximate solutions. The deviations of QA, TQA, and LN approximations from the "true" solution are minor, but the Born approximation fails. The next figure, Figure 3, presents the same approximate solutions but for an expanded vertical scale. We can see now the small differences between the various approximations.

To analyze more carefully the discrepancies in different approximations, we consider model 2 presented in Figure 1 (middle panel). In this experiment the transmitter (Tx) and receiver (Rx) geometry was fixed (transmitter-receiver separation was 100 m), with profiles run over the conductive prismatic body with the center at a depth of 35 m below the origin of x and y coordinates. For each position of the Tx/Rx system, we computed the vertical component of the magnetic field using the rigorous full IE method and three different approximations: (1) the QA approximation, (2) the LN approximation, and (3) the TQA approximation. The relative errors of approximate solutions in comparison with the rigorous solution were calculated as

$$\varepsilon = \frac{\|\mathbf{H}^{appr} - \mathbf{H}^{full}\|^2}{\|\mathbf{H}^{full}\|^2} \times 100\%. \qquad (37)$$

The main goal of this experiment is to demonstrate that the accuracy of approximation is not only a function of the conductivity contrast, frequency, and size of the anomalous body, it also depends on the relative locations of the transmitter, receiver and conductive target.

Figures 4, 5, and 6 are maps of relative errors for QA, LN, and TQA approximations correspondingly at the receiver for different positions of the recording system relative to the body center at a depth of 35 m below the earth's surface. Figure 7 shows the profiles of errors along the line connecting transmitter and receiver. One can see that for all three approximations the errors increase when the body is located just under the transmitter or the receiver. However, the largest discrepancies occur when the transmitter is near the inhomogeneity, with significantly lower (2–7%) discrepancies for all other locations. The most accurate result is delivered by TQA approximation (dotted line in Figure 7). The high level of discrepancies for
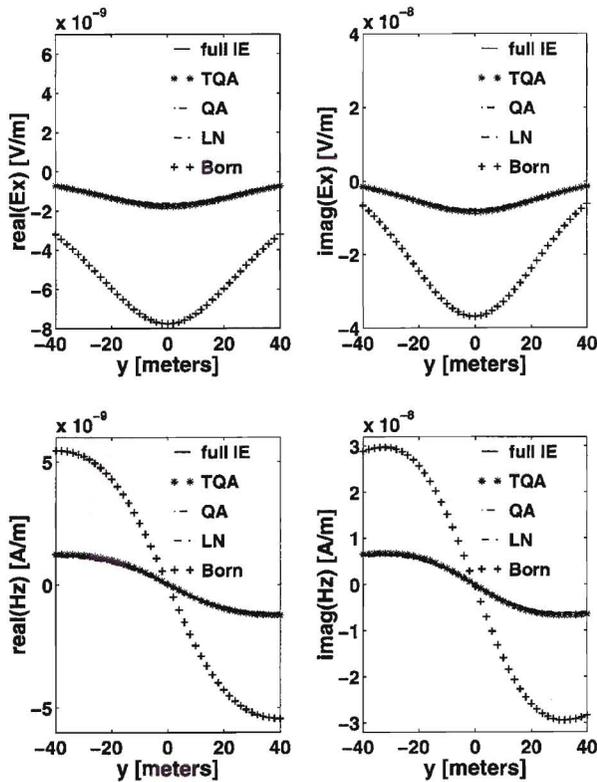
FIG. 2. Behavior of the anomalous electromagnetic field components computed for model 1 by solving the full integral equation, Born approximation, and the scalar QA, TQA, and LN approximations.
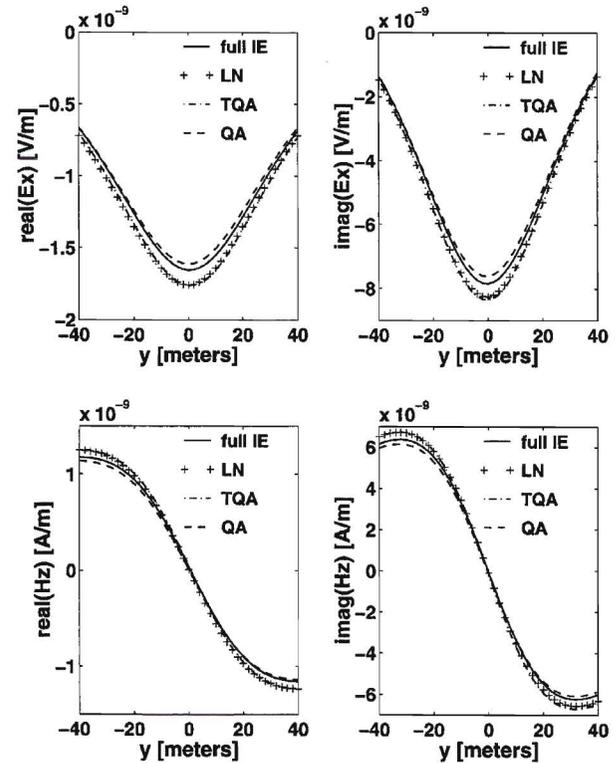
FIG. 3. Behavior of the anomalous electromagnetic field components computed for model 1 by solving the full integral equation, the scalar QA, TQA, and LN approximations.

QA approximation near the transmitter can be explained by the fact that the primary electric field is equal to zero on the vertical axes passing through the position of the transmitter dipole. Since the expression for scalar coefficient $g(\mathbf{r})$ in formulas (17) for the QA approximation becomes singular when $\mathbf{E}^b(\mathbf{r}) \to 0$, there is a significant increase of discrepancies in the near zone below the transmitter.

Another cause of discrepancies in this zone is the fact that QA approximation is based on a scalar reflectivity tensor. In the area below the transmitter, the primary electric field forms a "smoke ring" blown by the transmitting loop into the earth (Nabighian, 1979). The conductive body located just below the transmitter distorts this field through a secondary electric field, directed at some angle with the primary field. The scalar reflectivity tensor cannot account for this rotation of the sec-

ondary fields which generates additional discrepancies in the approximation. The plots in Figures 4–7 show that TQA and LN approximations handle this polarization pretty well. An especially accurate result is reached by a TQA solutions. The corresponding discrepancies do not exceed 7% and 15% in the areas under the receiver and transmitter, respectively.

An increase in discrepancies generated by LN approximation in comparison with TQA approximation can be explained by the fact that LN approximation is source independent. When the receiver is closer to the transmitter, the source effect becomes more significant, which leads to an increase in discrepancies. The TQA solution approximates the polarization of the secondary field and takes into account the source position. As a result, it produces a more accurate approximation, so the TQA approximation is source dependent.

$$\text{error} = |H^{QA} - H^{full}|_2 \,/\, |H^{full}|_2$$
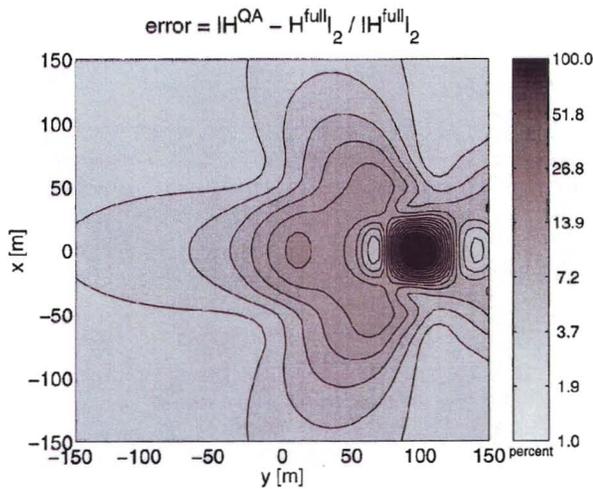
FIG. 4. Map of the relative errors between the scalar QA approximation and the full integral equation solution computed for model 2.

$$\text{error} = |H^{TQA} - H^{full}|_2 \,/\, |H^{full}|_2$$
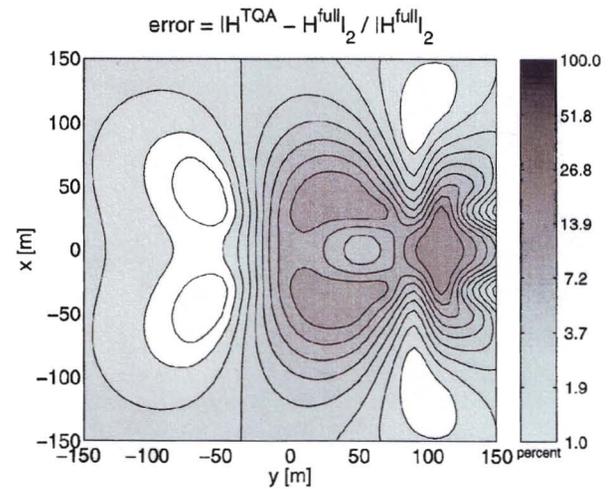
FIG. 6. Map of the relative errors between the tensor QA approximation and the full integral equation solution computed for model 2.

$$\text{error} = |H^{LN} - H^{full}|_2 \,/\, |H^{full}|_2$$
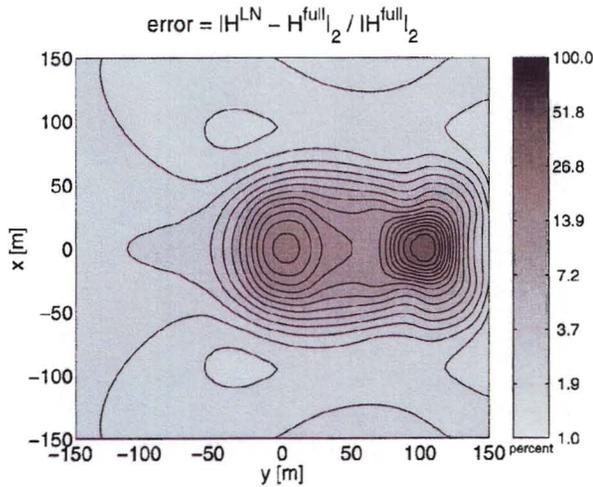
FIG. 5. Map of the relative errors between the LN approximation and the full integral equation solution computed for model 2.

Cross section of the error surfaces at y = 0
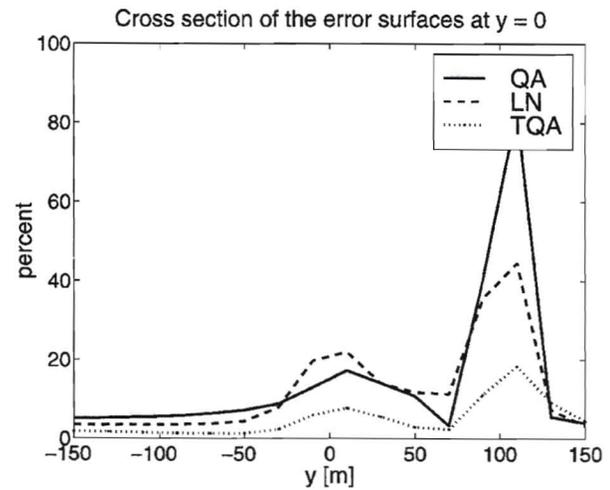
FIG. 7. The relative errors of the scalar QA approximation, TQA approximation, and LN approximations computed for model 2.

We analyzed also the effect of the conductivity contrast on the accuracy of different approximations. In Figure 8, we examine the relative errors for model 3 shown in Figure 1, bottom panel. The horizontal size of the conductive body in this model (100×100 m) is bigger than in model 2. The center of the conductive body is located just below the receiver. We consider now that the ratio of anomalous conductivity to background conductivity varies within a range of five orders of magnitude. One can see in the plot in Figure 8 that within a conductivity ratio range from 10^{-2} to 30, the best accuracy is provided by TQA approximations with the discrepancies less than 10%. For the higher conductivity ratio, the accuracy of all approximations becomes less than 20–30% .

Figures 9 and 10 illustrate the effect of frequency on the accuracy of approximation for model 3. The conductive rectangular prism has a resistivity of 1 ohm-m while the background resis-

tivity of a half-space is 10 ohm-m. The frequency range is from 10^{-1} up to 10^4 Hz. Figure 9 shows the ratio of the estimated to true (computed by IE method) amplitudes of the anomalous field H_z. Figure 10 presents the difference between the phases of the anomalous H_z component computed by true and approximate solutions.

The most significant feature of all these plots is the stable behavior of the QA approximation. The ratio of the approximated and true amplitudes of the anomalous field H_z is equal to one within the entire frequency range. The phase difference is also close to zero along the entire horizontal axis of the plot in Figure 10. At the same time both TQA and LN approximations produce good amplitude estimate till the frequency of 1 kHz, and good phases only for frequencies below 100 Hz. This similarity in the TQA and LN data behavior can be explained by the fact that both approximations are based on a depolarization tensor calculation, which is independent of the background field. Therefore, these approximations cannot take into account properly the background field which cause discrepancies in these approximations. At the same time, Figure 11 shows that at the frequency range above 100 Hz the induction effects become strong and the background field begins to vary significantly from its static limit. In the case of the QA approximation, we evaluate more carefully the induction effect because the background field is present in the expressions for scalar coefficient g in formulas (19) and (20) for QA anomalies. That is why the QA approximation produces stable results for a wide frequency range.

QUASI-ANALYTICAL SERIES

The main limitation of the QA method (as well as QL and LN approximations) is that it is still an approximate method of 3-D forward modeling, and its practical application requires additional control of the approximation discrepancies. It is possible, however, to increase the accuracy of the QA approximation by constructing QA approximations of a higher order in a similar
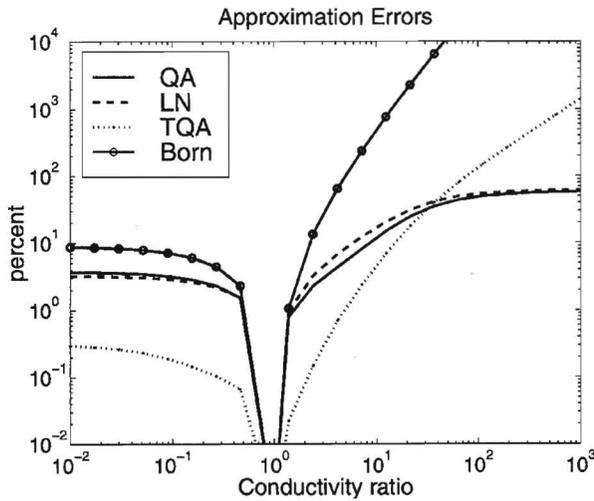
FIG. 8. The relative errors of different approximations as a function of the conductivity ratio computed for model 3.
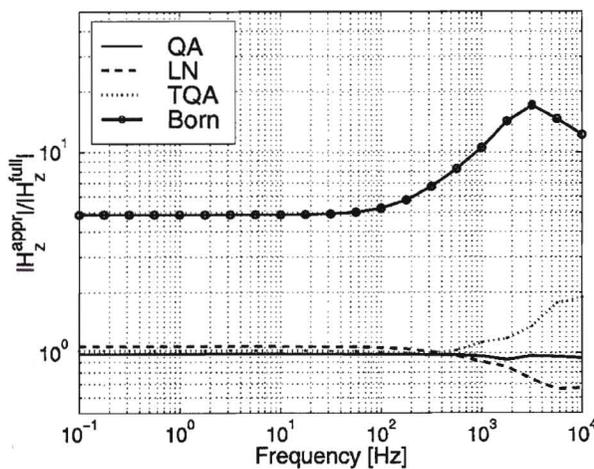
FIG. 9. The ratio of different approximations to the full integral equation solution of the scattered H_z as a function of frequency computed for model 3 with a conductivity of 10.
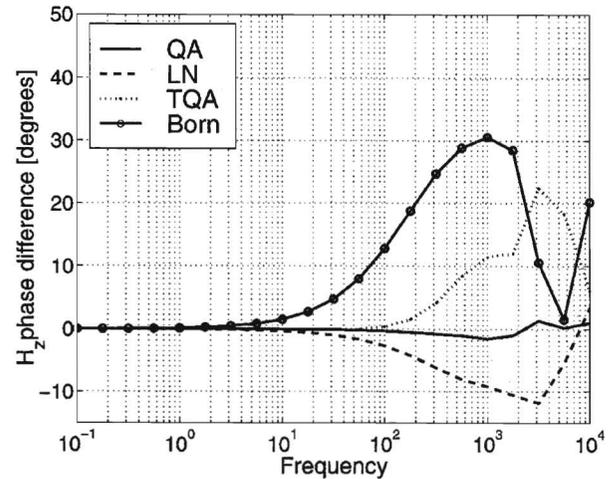
FIG. 10. The difference of the phases between the approximate and the full integral equation solutions of the scattered H_z as a function of frequency computed for model 3 with a conductivity of 10.

fashion to the QL series for QL approximations (Zhdanov and Fang, 1997).

The QL series were based on a new method of constructing the converged Born series developed by Singer and Fainberg (1995) and Pankratov et al. (1995). This method was applied in Zhdanov and Fang (1997) to construct QL series that almost always converged. In this paper, we use the same method to generate QA series and calculate the accuracy of the QA approximations. These series are built on the QA approximation as the first term of the series. As a result, the computation of QA series becomes even easier and faster than in the case of QL series, which required the solution of the linear algebraic equation in the first step of the iterations. Computation of the QA series does not involve any system of equation solution. It is based on repetitive application of the given integral contraction operator, which insures rapid convergence to the correct result.

Following Zhdanov and Fang, (1997) we modify Green's operator according to the formula

$$
\begin{aligned}
\mathbf{G}^m & (\Delta\tilde{\sigma}(\mathbf{r})\mathbf{E}^b(\mathbf{r})) \\
&= \sqrt{Re\tilde{\sigma}_b}\,\mathbf{G}_E(2\sqrt{Re\tilde{\sigma}_b}\Delta\tilde{\sigma}(\mathbf{r})\mathbf{E}^b(\mathbf{r})) + \Delta\tilde{\sigma}(\mathbf{r})\mathbf{E}^b(\mathbf{r}) \\
&= \sqrt{Re\tilde{\sigma}_b}\iiint_D \hat{\mathbf{G}}_E(\mathbf{r}_j\,|\,\mathbf{r})\,2\sqrt{Re\tilde{\sigma}_b}\Delta\tilde{\sigma}(\mathbf{r})\mathbf{E}^b(\mathbf{r})\,dv \\
&\quad + \Delta\tilde{\sigma}(\mathbf{r})\mathbf{E}^b(\mathbf{r}).
\end{aligned}
\tag{38}
$$

It was proved in Zhdanov and Fang (1997) that the L_2 norm of this operator is always less than or equal to one:

$$
\|\mathbf{G}^m\| \leq 1.
\tag{39}
$$

We can rewrite now the integral equation for the anomalous field (2) as follows:

$$
a\mathbf{E}^a = \mathbf{C}(a\mathbf{E}^a),
\tag{40}
$$

where $\mathbf{C}(a\mathbf{E}^a)$ is an integral operator of the anomalous field:

$$
\mathbf{C}(a\mathbf{E}^a) = \mathbf{G}^m[\beta a\mathbf{E}^a] + \mathbf{G}^m[\beta a\mathbf{E}^b] - \beta a\mathbf{E}^b,
\tag{41}
$$
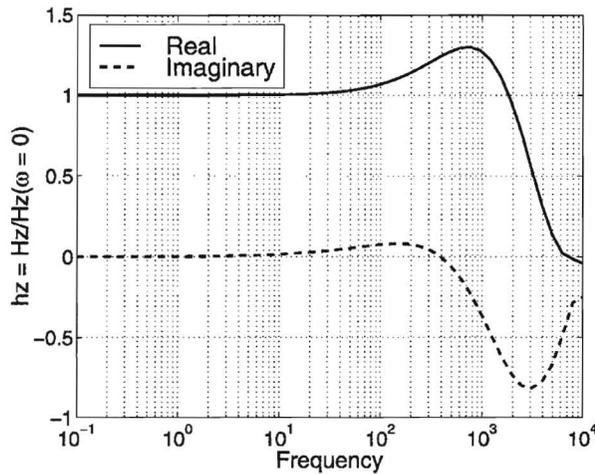
FIG. 11. Mutual coupling ratios of the real and imaginary parts of the vertical magnetic field over a homogeneous half-space of 10 ohm-m as a function of frequency.

and

$$
a = \frac{2Re\tilde{\sigma}_b + \Delta\tilde{\sigma}}{2\sqrt{Re\tilde{\sigma}_b}}, \qquad \beta = \frac{\Delta\tilde{\sigma}}{2Re\tilde{\sigma}_b + \Delta\tilde{\sigma}}.
$$

The solution of this integral equation can be obtained using the method of successive iterations, which is governed by the following equation:

$$
a\mathbf{E}^{a(N)} = \mathbf{C}[a\mathbf{E}^{a(N-1)}], \qquad N = 1, 2, 3 \ldots
\tag{42}
$$

These iterations always converge for any lossy medium because $\mathbf{C}$ is a contraction operator (Zhdanov and Fang, 1997).

We start iterations with the QA approximation for the anomalous field:

$$
\mathbf{E}_{qa}^{a(0)} = \frac{g}{1-g}\mathbf{E}^b.
\tag{43}
$$

In this case, the first order QA approximation is equal:

$$
\begin{aligned}
a\mathbf{E}_{qa}^{a(1)} = \mathbf{C}\big(a\mathbf{E}_{qa}^{a(0)}\big) &= \mathbf{G}^m\big[\beta a\mathbf{E}_{qa}^{a(0)}\big] \\
&\quad + \mathbf{G}^m[\beta a\mathbf{E}^b] - \beta a\mathbf{E}^b.
\end{aligned}
\tag{44}
$$

We will call the first iteration determined by expression (44) a *modified quasi-analytical approximation (MQA)*:

$$
\mathbf{E}_{qa}^{a(1)} = \mathbf{E}_{MQA}^a = \frac{1}{a}\mathbf{G}^m\big[\beta a\mathbf{E}_{qa}^{a(0)}\big] + \frac{1}{a}\mathbf{G}^m[\beta a\mathbf{E}^b] - \beta\mathbf{E}^b.
$$

Taking into account the definition of the modified Green's operator (38) and formula (43), we obtain

$$
\begin{aligned}
\mathbf{E}_{MQA}^a &= \frac{2Re\tilde{\sigma}_b}{2Re\tilde{\sigma}_b + \Delta\tilde{\sigma}}\big\{\mathbf{G}_E\big[\Delta\tilde{\sigma}\,\mathbf{E}_{qa}^{a(0)}\big] + \mathbf{G}_E\big[\Delta\tilde{\sigma}\mathbf{E}^b\big]\big\} \\
&= \frac{2Re\tilde{\sigma}_b}{2Re\tilde{\sigma}_b + \Delta\tilde{\sigma}}\mathbf{G}_E\left[\frac{\Delta\tilde{\sigma}}{1-g}\mathbf{E}^b\right] \\
&= \frac{2Re\tilde{\sigma}_b}{2Re\tilde{\sigma}_b + \Delta\tilde{\sigma}}\mathbf{E}_{MQA}^a.
\end{aligned}
\tag{45}
$$

Equation (45) shows that the modified QA approximation is equal to the original QA approximation outside inhomogeneity D:

$$
\mathbf{E}_{MQA}^a(\mathbf{r}_j) = \mathbf{E}_{QA}^a(\mathbf{r}_j), \mathbf{r}_j \notin D,
\tag{46}
$$

while they are different inside the geoelectrical inhomogeneity. The second-order QA approximation is equal to:

$$
\begin{aligned}
a\mathbf{E}_{qa}^{a(2)} = \mathbf{C}\big(a\mathbf{E}_{qa}^{a(1)}\big) &= (\mathbf{G}^m\beta)^2\big(a\mathbf{E}_{qa}^{a(0)}\big) \\
&\quad + \mathbf{G}^m(a\mathbf{E}^{Bm}) + a\mathbf{E}^{Bm},
\end{aligned}
$$

where $\mathbf{E}^{Bm}$ is a modified Born approximation determined by the formula

$$
\mathbf{E}^{Bm} = \frac{1}{a}\mathbf{G}^m\beta\mathbf{E}^b - \beta\mathbf{E}^b = \frac{2Re\tilde{\sigma}_b}{2Re\tilde{\sigma}_b + \Delta\tilde{\sigma}}\mathbf{E}^B.
$$

The third-order QA approximation is given by the formula

$$
\begin{aligned}
a\mathbf{E}_{qa}^{a(3)} = \mathbf{C}\big(a\mathbf{E}_{qa}^{a(2)}\big) &= (\mathbf{G}^m\beta)^3\big(a\mathbf{E}_{qa}^{a(0)}\big) + (\mathbf{G}^m\beta)^2(a\mathbf{E}^{Bm}) \\
&\quad + \mathbf{G}^m(a\mathbf{E}^{Bm}) + a\mathbf{E}^{Bm}.
\end{aligned}
$$

Finally, the Nth-order QA approximation can be treated as the sum of N terms of the QA series:

$$a\mathbf{E}_{qa}^{a(N)} = \sum_{k=0}^{N-1}(\mathbf{G}^m\beta)^k(a\mathbf{E}^{Bm}) + (\mathbf{G}^m\beta)^N\big(a\mathbf{E}_{qa}^{a(0)}\big), \quad (47)$$

where $\mathbf{G}^m$ is the modified Green's operator:

$$\begin{aligned}
&(\mathbf{G}^m\beta)\big(a\mathbf{E}_{qa}^{a(0)}\big)\\
&= \sqrt{Re\tilde{\sigma}_b}\iiint_D \hat{\mathbf{G}}_E(\mathbf{r}_j\,|\,\mathbf{r})\,2\sqrt{Re\tilde{\sigma}_b}b\mathbf{E}_{qa}^{a(0)}\,dv\\
&\quad + b\mathbf{E}_{qa}^{a(0)} = \sqrt{Re\tilde{\sigma}_b}\iiint_D \hat{\mathbf{G}}_E(\mathbf{r}_j\,|\,\mathbf{r})\Delta\tilde{\sigma}\mathbf{E}_{qa}^{a(0)}\,dv\\
&\quad + \frac{\Delta\tilde{\sigma}}{2\sqrt{Re\tilde{\sigma}_b}}\mathbf{E}_{qa}^{a(0)}(\mathbf{r}_j).
\end{aligned}$$

Note, that QA series can be built on TQA and LN approximations as the first iterations. We select the approach based on QA approximation for the sake of simplicity.

ACCURACY ESTIMATION

The accuracy of the QA approximation of the Nth order is estimated in the same way as in Zhdanov and Fang (1997) by the formula

$$\varepsilon_N = \frac{\left\| a\mathbf{E}^a - a\mathbf{E}_{qa}^{a(N)} \right\|}{\left\| a\mathbf{E}_{qa}^{a(N)} \right\|} \le \frac{\|\beta\|_\infty}{1-\|\beta\|_\infty}r_N, \qquad (48)$$

where $\mathbf{E}_{qa}^{a(0)} = \frac{ag}{1-g}\mathbf{E}^b$, and r_N is the relative convergence rate of the QA approximations:

$$r_N = \frac{\left\| a\mathbf{E}_{qa}^{a(N)} - a\mathbf{E}_{qa}^{a(N-1)} \right\|}{\left\| a\mathbf{E}_{qa}^{a(N)} \right\|}. \qquad (49)$$

In particular, the accuracy of the original QA approximation $\mathbf{E}_{QA}^a$ can be estimated by computing, using the formula

$$\varepsilon = \frac{\left\| a\mathbf{E}^a - a\mathbf{E}_{QA}^a \right\|}{\left\| a\mathbf{E}_{QA}^a \right\|} \le \frac{\|\beta\|_\infty}{1-\|\beta\|_\infty} \cdot \frac{\left\| a\mathbf{E}_{QA}^a - \frac{ag}{1-g}\mathbf{E}^b \right\|}{\left\| a\mathbf{E}_{QA}^a \right\|}. \qquad (50)$$

Thus, the accuracy estimation formula for QA solutions is expressed by the QA solution itself.

Formulas (48) and (50) make it possible to obtain a quantitative estimation of the QL approximation accuracy without direct comparison with the rigorous full IE forward modeling solution.

NUMERICAL MODELING RESULTS

We developed a computer code based on the QA series for the electromagnetic field in a 3-D case. The algorithm was tested for 3-D geoelectrical models.

Consider a 3-D geoelectrical model (model 4), consisting of a homogeneous half-space (with resistivity of 100 ohm-m) and a thin conductive rectangular inclusion with the resistivity of 1 ohm-m (Figure 12). The electromagnetic field in this model is excited by a horizontal rectangular loop, located 50 m to the left of the model, with the loop 10 m on a side and a current of 1 A. We have used the integral equation code for computing the scattering current in the complex conductivity structure and the QA series code.

Figure 13 presents maps of the excess electrical currents distribution within the inhomogeneity obtained by a rigorous

Model 4
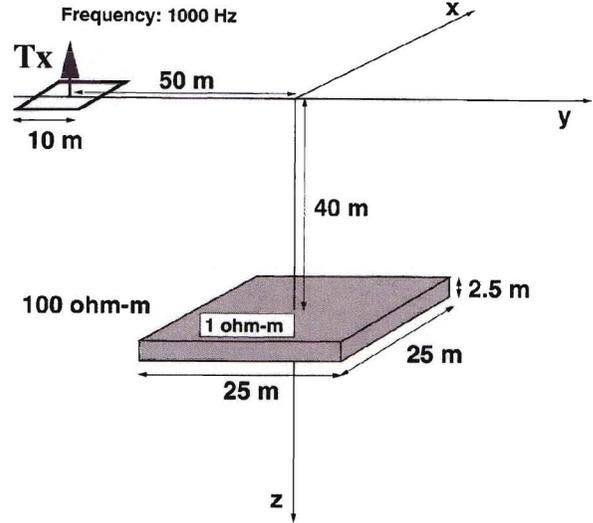
FIG. 12. 3-D geoelectrical model of a thin conductive rectangular body embedded in a homogeneous half-space excited by a horizontal rectangular loop (model 4).
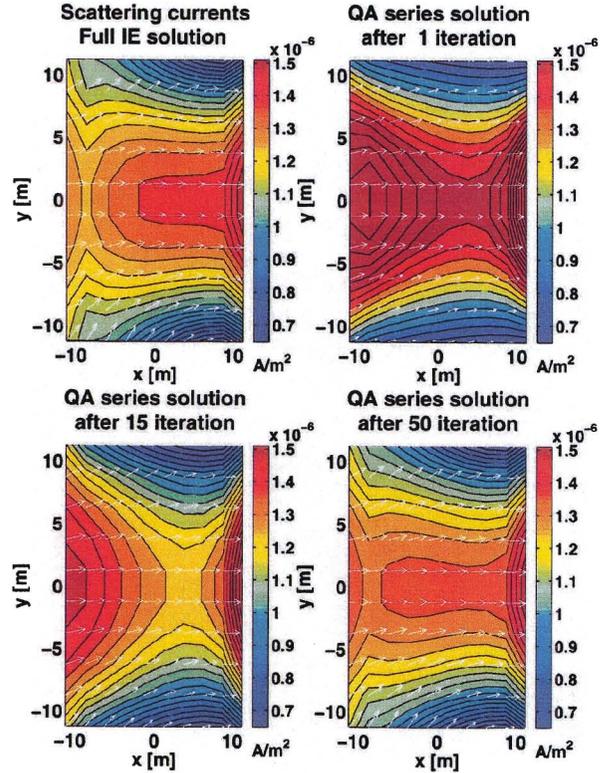
FIG. 13. Behavior of the scattering currents induced inside the conductive rectangular body in model 4 obtained by solving the full integral equation and the approximate solution after one, 15, and 50 iterations.

integral equation solution and by QA series of different orders for a frequency of 1000 Hz. Note that this model is a difficult one for QA approximation because it contains a conductivity contrast of 100. Nevertheless, we can see how the currents computed by QA series converge to the true solution. Figure 14 presents a map of relative errors in the excess current calculations between the integral equation technique and the QA series of the order of 5 and 15. One can observe that the discrepancies decrease during the iterations.

We applied the QA series solution to model the EM response for the more complicated model simulating the Kambalda-style nickel sulfide deposit in Western Australia (Stolz et al., 1995.). The sketch of the model is shown in the top panel of Figure 15; the bottom panel of Figure 15 shows the vertical geoelectrical cross-section of the model. The model consists of a conductive overburden above an inclined nickel lens. The conductivity contrast between the nickel lens and the host rocks is 10^4, which is far beyond the normal limits of QA approximations. Figure 16 presents the horizontal and vertical anomalous magnetic fields of forward modeling based on integral equation solution and QA series of the order of 1, 10, 20, and 50. The very high conductivity contrast and the proximity of the anomalous body causes inaccuracies in the approximate solutions. However, the always convergent series algorithm provides the correct values.

Table 1 shows a comparison of CPU time for EM modeling using integral IE (Xiong, 1992) and the QA approximations of the different orders for the thin sheet and the Kambalda-style nickel-sulfide deposit models. For 1088 cells and 50 iterations

of the QA series, the algorithm spent approximately half the CPU time required for the solution of the full integral equation. For 4352 cells, the time gain is very significant. It takes about 2.5 hours for the new code to run 50 iterations, which generates the same solution as the integral equation code (Figure 16). It took more than five days to reach the same result using full IE method.

CONCLUSION

We have generalized the QL method of forward modeling and developed a new approach to calculation of the electrical

Table 1. Comparison of the CPU time (in seconds) for EM modeling using full integral equation solution and QA approximations of the different orders for the thin sheet and the Kambalda-style nickel-sulfide deposit models.

Cells Cells	Full IE Full IE	1st-order QA	20th-order QA	50th-order QA
100	30	11	15	21
1088	1264	221	368	589
2176	21 687	459	1326	2967
4352	490 752	911	3931	8827

3-D ore deposit model

FIG. 15. Kambalda-style ore deposit model with an inclined dike structure. The bottom panel shows the vertical resistivity cross-section.

Relative error after 5 iterations

Relative error after 15 iterations

FIG. 14. Maps of the relative residuals of scattering currents obtained by different orders of QA series with respect to the full integral equation solution. The number of iterations is 5 (top) and 15 (bottom).
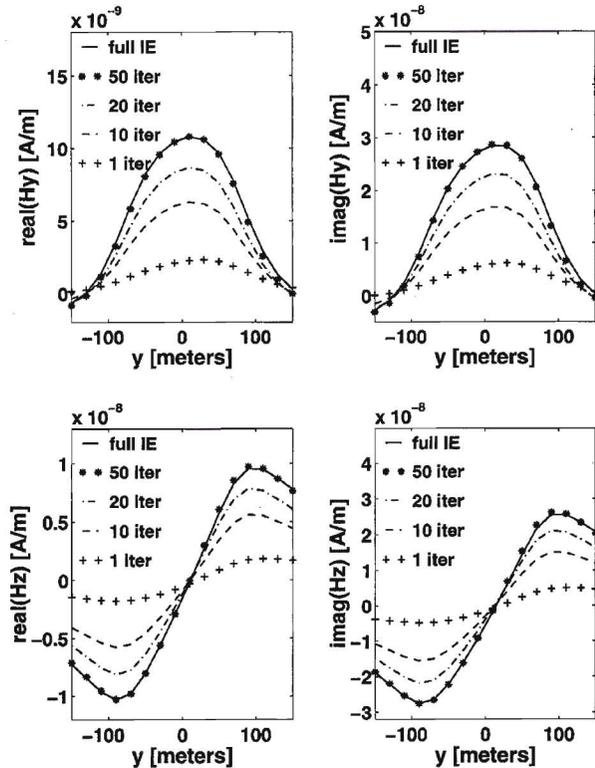
FIG. 16. Magnetic field components obtained by different numbers of iterations of QA series and full integral equation solutions over the Kambalda-style ore deposit model.

reflectivity tensor based on the solution of the corresponding integral equation.

Based on this approach, we introduced the new scalar (QA) and tensor (TQA) quasi-analytical solutions for electromagnetic fields in 3-D inhomogeneous media. We demonstrated also that TQA approximation is a generalization of the localized nonlinear approximation introduced by Habashy et al. (1993). The new TQA approximation permits different polarizations for the background and anomalous (scattered) field, which increases the accuracy of approximation for conductivity contrasts below 30. The comparative accuracy study of the different approximations demonstrates that TQA approximation has a superb accuracy, especially in the areas close to the transmitter and to the anomalous geoelectrical structures. At the same time, QA approximation generates a stable and accurate result (discrepancies below 3%) for a wide frequency range (from 10^{-1} up to 10^4 Hz).

The computational time for QA approximations is comparable with that required for the Born approximation, although the new approximate solutions are much more accurate. To generate a rigorous forward-modeling result, we may apply these approximations iteratively. This approach leads us to a construction of the QA series.

The developed approximations of the electromagnetic field can be used as effective tools for fast 3-D forward modeling. One of the attractive areas of their application is rapid computing of the Fréchet derivative for 3-D electromagnetic inversion.

We improved the accuracy of the QA approximation by constructing QA approximations of a higher order in a similar way as has been done for QL approximations in Zhdanov and Fang (1997). These series are a new fast and accurate method of 3-D EM modeling that accelerate dramatically the solution of forward EM problems in inhomogeneous 3-D geoelectrical structures.

REFERENCES

Dmitriev, V. I., and Pozdnyakova, E. E., 1992, Method and algorithm for computing the electromagnetic field in stratified medium with a local inhomogeneity in an arbitrary layer: Computational Mathematics and Modeling, **3**, 181–188.
Dmitriev, V. I., Pozdnyakova, E. E., Zhdanov, M. S., and Fang, S., 1998, Quasi-analytical solutions for the EM field in inhomogeneous structures based on a unified iterative quasi-linear method: 68th Ann. Mtg., Soc. Expl. Geophys., Expanded Abstracts, 444–447.
Dmitriev, V. I., and Sedelnikova, A. V., 1992, Iterative method for computing the anomalous electric field in a conducting medium: Computational Mathematics and Modeling, **3**, 197–203.
Habashy, T. M., Groom, R. W., and Spies, B. R., 1993, Beyond the Born and Rytov approximations: A nonlinear approach to electromagnetic scattering: J. Geophys. Res., **98**, B2, 1759–1775.
Hohmann, G. W., 1975, Three-dimensional induced polarization and EM modeling: Geophysics, **40**, 309–324.
Nabighian, M. N., 1979, Quasi-static transient response of a conducting half-space—An approximate representation: Geophysics, **44**, 1700–1705.
Pankratov, O. V., Avdeev, D. B., and Kuvshinov, A. V., 1995, Scattering of electromagnetic field in inhomogeneous earth. Forward problem solution: Fizika Zemli, No. 3, 17–25.
Singer, B. S., and Fainberg, E. B., 1995, Generalization of iterative dissipative method for modeling electromagnetic fields in nonuniform media with displacement currents: J. Appl. Geophys., **34**, 41–46.
Stolz, N., Raiche, A., Sugeng, F., and Macnae, J., 1995, Is full 3-D inversion necessary for interpreting EM data?: Expl. Geophys., **26**, 167–171.
Torres-Verdin, C., and Habashy, T. M., 1994, Rapid 2.5-dimensional forward modeling and inversion via a new nonlinear scattering approximation, Radio Sci., **29**, 1051–1079.
Weidelt, P., 1975, EM induction in three-dimensional structures: J. Geophysics, **41**, 85–109.
Xiong, Z., 1992, EM modeling of three-dimensional structures by the method of system iteration using integral equations: Geophysics, **57**, 1556–1561.
Zhdanov, M. S., and Fang, S., 1996a, Quasi-linear approximation in 3-D EM modeling: Geophysics, **61**, 646–665.
——1996b, 3-D quasi-linear electromagnetic inversion: Radio Sci., **31**, 741–754.
——1997, Quasi-linear series in 3-D EM modeling: Radio Sci., **32**, 2167–2188.

APPENDIX A
ITERATIVE METHOD

We demonstrate here that approximate expressions (16) and (22) for the electrical reflectivity tensor can be treated as the first iterations within an iterative solution of the TQL equation (8) solution.

Let us subtract $\mathbf{G_E}[\Delta\tilde{\sigma}\hat{\lambda}(\mathbf{r_j})\mathbf{E^b}]$ from both sides of equation (8):

$$\hat{\lambda}(\mathbf{r_j})\mathbf{E^b}(\mathbf{r_j}) - \mathbf{G_E}[\Delta\tilde{\sigma}\hat{\lambda}(\mathbf{r_j})\mathbf{E^b}]$$
$$= \mathbf{G_E}[\Delta\tilde{\sigma}(\hat{\lambda}(\mathbf{r}) - \hat{\lambda}(\mathbf{r_j}))\mathbf{E^b}] + \mathbf{E^B}(\mathbf{r_j}). \quad \text{(A-1)}$$

One can apply an iterative process to solve equation (A-1):

$$\hat{\lambda}^{(k+1)}(\mathbf{r_j})\mathbf{E^b}(\mathbf{r_j}) - \mathbf{G_E}[\Delta\tilde{\sigma}\hat{\lambda}^{(k+1)}(\mathbf{r_j})\mathbf{E^b}]$$
$$= \mathbf{G_E}[\Delta\tilde{\sigma}(\hat{\lambda}^{(k)}(\mathbf{r}) - \hat{\lambda}^{(k)}(\mathbf{r_j}))\mathbf{E^b}] + \mathbf{E^B}(\mathbf{r_j}), \quad \text{(A-2)}$$

where k is the iteration number and

$$\hat{\lambda}^{(0)}(\mathbf{r}) = 0. \quad \text{(A-3)}$$

Note that convergence of this iteration process for a specific geoelectrical model depends on the properties of the operator

$$A[\hat{\lambda}(\mathbf{r}) - \hat{\lambda}(\mathbf{r_j})] = \mathbf{G_E}[\Delta\tilde{\sigma}(\hat{\lambda}(\mathbf{r}) - \hat{\lambda}(\mathbf{r_j}))\mathbf{E^b}]. \quad \text{(A-4)}$$

It was demonstrated by Dmitriev and Sedelnikova (1992) that the L_2 norm of this operator determined on a class of the slowly varying functions is usually small, which provides the convergence of the iteration process (A-2). This assumption is based on the fact that for slowly varying $\hat{\lambda}(\mathbf{r})$, the difference $[\hat{\lambda}(\mathbf{r}) - \hat{\lambda}(\mathbf{r_j})]$ is small if $\mathbf{r_j}$ is close to $\mathbf{r}$, and the kernel $\hat{\mathbf{G}}_E(\mathbf{r_j}\,|\,\mathbf{r})$ is small if the distance between the points $\mathbf{r_j}$ and $\mathbf{r}$ is large. In other words, one can consider that operator $A[\hat{\lambda}(\mathbf{r}) - \hat{\lambda}(\mathbf{r_j})]$, acting on the class of slow varying functions, is a small operator (has a small L_2 norm).

We demonstrated that by using a modified Green's operator with the norm less or equal to one (Zhdanov and Fang, 1997), we can construct the modified tensor QL equation with the norm of the operator $A[\hat{\lambda}(\mathbf{r}) - \hat{\lambda}(\mathbf{r_j})]$ always small. So, in this situation, the iterative process (A-2) will always converge.

In the case of a scalar electrical reflectivity tensor, integral equation (A-1) can be rewritten as

$$\lambda(\mathbf{r_j})[\mathbf{E^b}(\mathbf{r_j}) - \mathbf{E^B}(\mathbf{r_j})]$$
$$= \mathbf{G_E}[\Delta\tilde{\sigma}(\lambda(\mathbf{r}) - \lambda(\mathbf{r_j}))\mathbf{E^b}] + \mathbf{E^B}(\mathbf{r_j}). \quad \text{(A-5)}$$

Calculating the dot product of both sides of equation (A-5) and the background electric field, and dividing the resulting equation by the square of the background field, we obtain

$$\lambda(\mathbf{r_j})[1 - \mathbf{g}(\mathbf{r_j})] = A[\lambda^{(k)}(\mathbf{r}) - \lambda^{(k)}(\mathbf{r_j})] + g(\mathbf{r_j}), \quad \text{(A-6)}$$

where $g(\mathbf{r_j})$ is determined by equation (17), and

$$A[\lambda(\mathbf{r}) - \lambda(\mathbf{r_j})] = \frac{\mathbf{G_E}[\Delta\tilde{\sigma}(\lambda(\mathbf{r}) - \lambda(\mathbf{r_j}))\mathbf{E^b}] \cdot \mathbf{E^b}(\mathbf{r_j})}{\mathbf{E^b}(\mathbf{r_j}) \cdot \mathbf{E^b}(\mathbf{r_j})}. \quad \text{(A-7)}$$

The integral equation (A-6) can also be solved iteratively:

$$\lambda^{(k+1)}(\mathbf{r_j})[1 - \mathbf{g}(\mathbf{r_j})] = A[\lambda^{(k)}(\mathbf{r}) - \lambda^{(k)}(\mathbf{r_j})] + g(\mathbf{r_j}). \quad \text{(A-8)}$$

As we already discussed above, these iterations will converge to a true solution due to the small norm of operator $A[\lambda(\mathbf{r}) - \lambda(\mathbf{r_j})]$ acting on the class of slowly varying functions. Note that these iterations will always converge if one uses the modified Green's operator in equation (A-7).

The first iteration of equation (A-8) yields

$$\lambda^{(1)}(\mathbf{r_j}) = \frac{g(\mathbf{r_j})}{1 - g(\mathbf{r_j})}, \quad \text{(A-9)}$$

which coincides with the approximate formula (16).

Thus, we can see that QA approximation can be treated as the first iteration in the solution of the TQL equation using the iterative algorithm (A-8).

Note that in the same way one can demonstrate that TQA approximation can be treated as the first iteration in the iterative solution of the TQL equation for tensor $\hat{\lambda}(\mathbf{r})$.